G.Y. Bharate, J. Fang, H. Nakamura, H. Qin, S. Shinkai, and H. Maeda	4-Amino-6- hydroxypyrazolo [3,4-d] pyrimidine (AHPP) conjugated PEG micelles: Water soluble polymeric xanthine oxidase inhibitor.	J. Drug. Targeting	19	954-66	2011
N. Larson, K. Greish, H. Bauer, H. Maeda, H. Ghandehari	Synthesis and evaluation of poly(styrene-co-maleic acid) micellar nanocarriers for the delivery of tanespimycin.	Int'l. J. Pharmaceutics	420	111-7	2011
J. Fang, H. Qin, T. Seki, H. Nakamura, K. Tsukigawa, H. Maeda	Therapeutic potential of pegylated hemin for ROS-related diseases via induction of heme oxygenase-1: results from a rat hepaticischemia/reperfusion injury model.	J. Pharmacol. Exp. Ther.	339	779-89	2011
H. Nakamura, J. Fang, H. Maeda	Protective Role of D-Amino Acid Oxidase Against Bacterial Infection.	Infection and Immunity	80	1546-53	2012
H. Herrmann, M. Kneidinger, S. Cerny-Reiterer, T. Rülicke, M. Willmann, K.V. Gleixner, K. Blatt, G. Hörmann, B. Peter, P. Samorapoompichit, W. Pickl, G. Y. Bharate, M. Mayerhofer, W. R. Sperr, H. Maeda, P. Valent	The Hsp32 inhibitors SMA-ZnPP and PEG-ZnPP exert major growth-inhibitory effects on $CD34^{+}/CD38^{+}$ and $CD34^{+}/CD38^{-}$ AML progenitor cells.	Current Cancer Drug Targets	12 (1)	51-63	2012
H. Maeda	Vascular permeability in cancer and infection as related to macromolecular drug delivery, with emphasis on the EPR effect for tumor-selective drug targeting.	Proc. Jpn. Academy, Series B.	88	53-71	2012
G. Bharate, H. Nakamura, J. Fang, S. Shinkai, H. Maeda	Styrene-co-maleic Acid (SMA) Telomeric Micelles Encapsulated-Zinc Protoporphyrin (SMA-ZnPP) and Other Drugs: Stability Study.	CRS Newsletter	29	6-7	2012
J. Fang, H. Qin, H. Nakamura, K. Tsukigawa, H. Maeda	Carbon monoxide, generated by heme oxygenase-1, mediates the enhanced permeability and retention (EPR) effect of solid tumor.	Cancer Science	102	535-41	2012

J. Fang, K. Greish, H. Qin, H. Nakamura, M. Takeya, H. Maeda	HSP32 (HO-1) inhibitor, copoly(styrene-maleic acid)-zinc protoporphy- rin IX, a water-soluble micelle as anticancer agent: In vitro and in vivo anticancer effect.	Eur. J. Pharm. Biopharma.	81	540-7	2012
H. Nakamura, J. Fang, T. Mizukami, H. Nunoi, H. Maeda	Pegylated D-amino acid oxidase restores bactericidal activity of neutrophils in chronic granulomatous disease via hypochlorite	Exp. Biol. Med.	237	703-8	2012
Y. Ishima, D. Chen, J. Fang, H. Maeda, A. Minomo, U. Kragh-Hansen, T. Kai, T. Maruyama, M. Otagiri	S-Nitrosated human serum albumin dimer is not only a novel anti-tumor drug but also a potentiator for snti-tumor drugs with augmented EPR effects	Bioconjug. Chem	23	264-71	2012
H. Maeda	Macromolecular therapeutics in cancer treatment: the EPR effect and beyond,	J. Control. Release	164	138-44	2012
前田 浩	EPR効果に基づく腫瘍のターゲッティングと蛍光イメージング	Progress in Drug Delivery System XXI（2012年9月1日開催静岡DDSカンファレンス抄録）		5-12	2012
H. Nakamura, L. Liao, Y. Hitaka, K. Tsukigawa, V. Subr, J. Fang, K. Ulbrich, H. Maeda	Micelles of zinc protoporphyrin conjugated to *N*-(2-hydroxypropyl) methacrylamide (HPMA) copolymer for imaging and light-induced antitumor effects in vivo.	J. Control. Release	165	191-8	2013
H. Maeda, H. Nakamura, J. Fang	The EPR effect for macromolecular drug delivery to solid tumors: improved tumor uptake, less systemic toxicity, and improved tumor imaging －Review of the vascular permeability of tumors and the EPR effect.	Adv. Drug Deliver. Rev	65	71-9	2013
U. Prabhakar, H. Maeda, R. K. Jain, E. Sevick-Muraca, W. Zamboni, O.C. Farokhzad, S.T. Barry, A. Gabizon, P. Grodzinski, D.C. Blakey,	Challenges and key considerations of the enhanced permeability and retention effect (EPR) for nanomedicine drug delivery in oncology.	Cancer Res.	73	2412-7	2013
S. Yamamoto, Y. Kaneo, H. Maeda	Styrene maleic acid anhydride copolymer (SMA) for the encapsulation of sparingly water-soluble drugs in nanoparticles.	J. Drug Del. Sci. Tech.	23	231-7	2013

H. Maeda	The link between infection and cancer: Tumor vasculature, free radicals, and drug delivery to tumors via the EPR effect.	Cancer Sci.	104	779-89	2013
J. Fang, T. Seki, T. Tetsuya, H. Qin, H. Maeda,	Protection from inflammatory bowel disease and colitisassociated carcinogenesis with 4-vinyl-2, 6-dimethoxyphenol (canolol) via suppression of oxidative stress	Carcinogen.	34	2833-41	2013
J.H. Grossman, S. McNeil ［翻訳］H. Maeda	Nanotechnology in Cancer Medicine, Physics Today 65, 38-42 (2012) 「がん治療におけるナノテクノロジー」	パリティ誌、丸善書店			2013 8月号
H. Nakamura, T. Etrych, P. Chytil, M. Ohkubo, J. Fang, K. Ulbrich, H. Maeda	Two step mechanisms of tumor selective delivery of N-(2-hydroxypropyl)methacrylamide copolymer conjugated with pirarubicin via an acid-cleavable linkage. —23—	J. Control. Release	174	81-7	2014
S. Cerny-Reiterer, R. A. Meyer, H. Herrmann, B. Peter, K. V. Gleixner, G. Stefanzl, E. Hadzijusufovic, W. F. Pickl, W. R. Sperr, J. V. Melo, H. Maeda, U. Jäger, P. Valent	Identification of heat shock protein 32 (Hsp32) as a novel target in acute lymphoblastic leukemia.	Oncotarget.			Online Mar.4, 2014
H. Yin, J. Fang, L. Liao, H. Nakamura, and H. Maeda	Styrene-maleic acid copolymer-encapsulated CORM2, a water-soluble carbon monoxide (CO) donor with a constant CO-releasing property, exhibits therapeutic potential for inflammatory bowel disease.	J. Control Release			in press, 2014
H. Maeda	Analysis of the causes of failures in cancer chemotherapy and improvements for tumor-selective drug delivery, therapeutic efficacy, and eliminating adverse effects.	Proc. Jpn. Academy Ser. B			in press, 2014
H. Maeda	Emergence of EPR effect theory and development of clinical applications for cancer therapy.	Therapeutic Delivery (Future Science)			in press, 2014
H. Nakamura, J. Fang, H. Maeda	Macromolecular cancer drug development for next generation drugs based on the EPR effect: challenges and pitfalls	Expert Opinion on Drug Delivery			in press, 2014

H. Nakamura, E. Koziolová, T. Etrych, P. Chytil, J. Fang, K. Ulbrich, H. Maeda	Improved pharmacokinetics and antitumor activity of new dendrimer-derived poly(*N*-(2-hydroxypropyl) methacrylamide) conjugates of pirarubicin	Eur. J. Pharm. Biopharm.			in press, 2014
Y. Ishima, J. Fang, Ulrich Kragh-Hansen, H. Yin, L. Liao, N. Katayama, H. Watanabe, T. Kai, A. Suenaga, H. Maeda, M. Otagiri, and T. Maruyama	Tuning of Poly-*S*-Nitrosated Human Serum Albumin as Superior Antitumor Nanomedicine.	J. Pharm. Sci.			in press, 2014
中村 秀明、方 軍、前田 浩	EPR効果に基づくポリマー抗癌剤の腫瘍デリバリー：微小癌の検出・治療を目的としたセラノスティック薬剤の開発	月刊「化学工業」			in press, 2014 6月号
J. Fang, L. Liao, H. Yin, H. Namamura, T. Shin, H. Maeda	nhanced bacterial tumor delivery by modulating the EPR effect, and therapeutic potential of *Lactobacillus casei*	J. Pharm. Sci.			Submitted, 2014
前田 浩	現今のがん治療薬のかかえる問題	公益財団法人札幌がんセミナー会報　SCSコミュニケーションThe Way Forward			in press, 2014

研究成果の刊行物・別刷

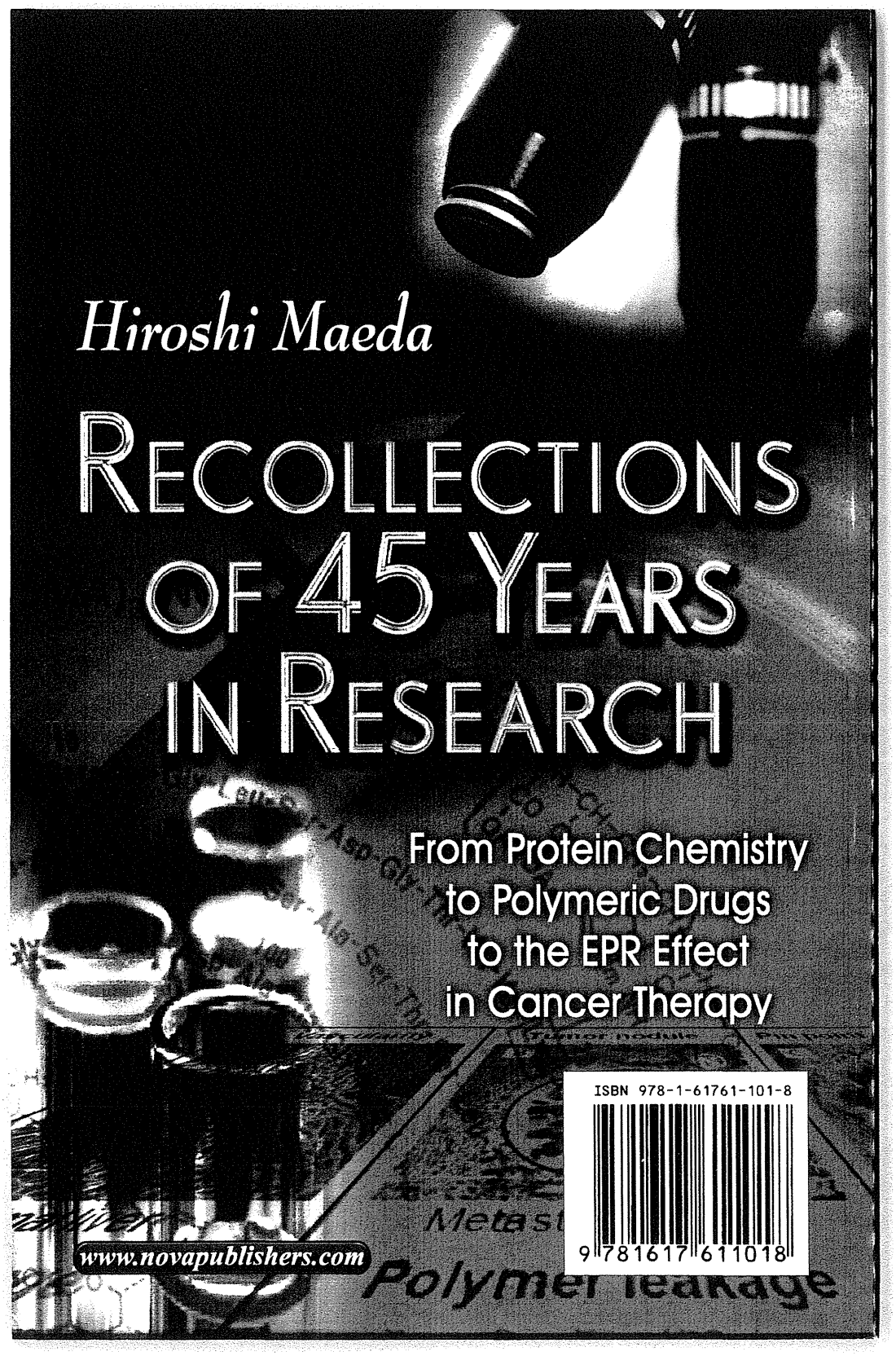
Hiroshi Maeda
RECOLLECTIONS OF 45 YEARS IN RESEARCH
From Protein Chemistry to Polymeric Drugs to the EPR Effect in Cancer Therapy
www.novapublishers.com
ISBN 978-1-61761-101-8
9 781617 611018
Polymer leakage

In: Science Education in a Rapidly Changing World
Editor: Seth D. Grahame
ISBN 978-1-61728-914-9

Chapter 1

RECOLLECTIONS OF 45 YEARS IN RESEARCH: FROM PROTEIN CHEMISTRY TO POLYMERIC DRUGS TO THE EPR EFFECT IN CANCER THERAPY

Hiroshi Maeda*
Laboratory of Microbiology and Oncology, Faculty of Pharmaceutical Sciences, and
Division of Applied Chemistry,
Graduate School of Engineering,
Sojo University, Kumamoto, 860-0082 Japan

ABSTRACT

This article describes the lifelong research experience of a scientist, from the beginning studies of protein chemistry to development of a protein drug (neocarzinostatin, NCS) to the invention of the first polymer conjugate drug—poly(styrene-co-maleic acid (SMA) conjugated to NCS, —called SMANCS. The author, having acquired knowledge of proteases and inhibitors, pioneered investigations of microbial proteases in the pathogenesis of bacterial infection. The author's group, using a polymer-conjugated enzyme (superoxide dismutase), discovered an enormous burst in the generation of superoxide anion radical ($O_2^{\cdot -}$) during influenza virus infection by the generation of xanthine oxidase. $O_2^{\cdot -}$ was found to be the major cause of the pathogenesis of this viral infection, which progressed even after the virus was eradiated. These events can be interpreted as advancing beyond the boundary of Robert Koch's postulates, that is, *viral disease occurring in the absence of virus*. Also, the importance of endogenous free radicals, now referred to as reactive oxygen species (ROS) and reactive nitrogen species (RNS), during the microbial infections. Role of ROS and RNS in human disease and health became clear, in that they were crucial factors for development of (eg. drug-resistant mutant) formation of mutant microorganisms in chronic and acute infections as well ass carcinogenesis.

* Corresponding author. Tel.: +81 96-326-4114; fax: +81 96-326-4114. E-mail address: hirmaeda@ph.sojo-u.ac.jp.

3
Enhanced Permeability and Retention Effect in Relation to Tumor Targeting

Hiroshi Maeda

3.1
Background and Status Quo

We first described the enhanced permeability and retention (EPR) effect of macromolecules in solid tumors under the title of "A new concept for macromolecular therapeutics in cancer chemotherapy: mechanism of tumoritropic accumulation of proteins and the antitumor agent SMANCS" in the December 1986 issue of *Cancer Research* [1]. In prior publications we had described the relationship of plasma half-life of small proteins of about 10 kDa to more than 240 kDa as well as the biocompatibility of proteins in relation to the conformational integrity. For instance, the native versus denatured form of α_2-macroglobulin shows a drastic reduction of plasma half-life when this plasma protease inhibitor of 240 kDa complexes with a protease (trypsin) due to rapid uptake by phagocytotic cells or hepatic entrapment [2–4]. Obviously, inadequate chemical modifications of biocompatible plasma or other proteins will reduce plasma half-life, while appropriate modifications will prolong their half-lives. This effect was noted for the modification of many proteins (e.g., superoxide dismutase (30 kDa) and ribonuclease (12.5 kDa) with divema (divinyl ether–maleic acid copolymer or pyran copolymer), neocarzinostatin (NCS) (12 kDa) with styrene–maleic acid copolymer (SMA) or poly(ethylene glycol) (PEG), etc.) [2–5]. In addition to plasma half-life, two crucial points should be emphasized. Namely, all plasma and other proteins of molecular weight above 40 kDa exhibited tumor-selective accumulation. Thus, we envisaged preferential drug targeting to solid tumors by using macromolecular drugs [1, 2]. We also noted that such macromolecular derivatives accumulated preferentially in the lymphatic tissues [6–8]. The latter point has not received enough attention among oncologists or in the field of cancer chemotherapy, regardless of its importance in relation to lymphatic metastases. Namely, many therapeutic failures in cancer chemotherapy can be attributed to the failure of controlling lymphatic metastases. As a matter of fact, there is no effective treatment for lymphatic metastases, and therapy with common anticancer drugs without lymphotropic accumulation does not control the growth and spread of lymphatic metastases [6–10].

Drug Delivery in Oncology: From Basic Research to Cancer Therapy, First Edition.
Edited by Felix Kratz, Peter Senter, and Hemming Steinhagen.

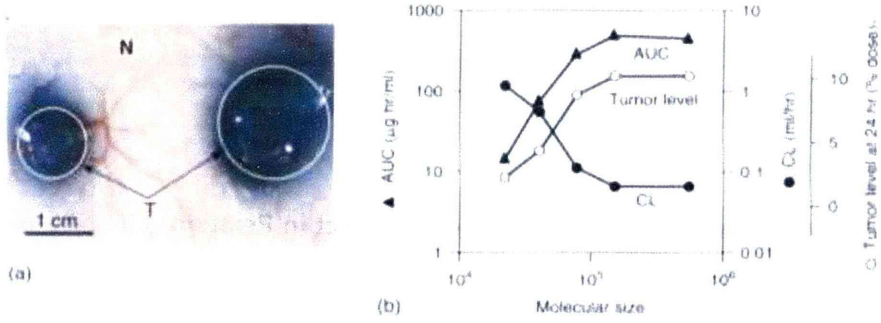

Figure 3.1 (a) EPR effect visualized in experimental mouse tumors where albumin-bound Evans blue (molecular weight 68 kDa) is selectively accumulated only in subcutaneously growing tumor. Arrows 'T' pointing to blue spots are tumors. 'N' is the normal skin that shows no vascular leakage (in contrast to blue-stained tumor). Accumulated Evans blue will remain in the tumor for more than 2–3 weeks. (b) Relation between molecular weight of drugs, plasma level (area under the concentration curve (AUC)), tumor concentration, and renal clearance rate (CL). (Data from [13].)

We have elaborated the EPR effect further by using another biocompatible synthetic polymer, *N*-(2-hydroxypropyl)methacrylamide (HPMA) copolymers, with discrete molecular size distributions, which were supplied by K. Ulbrich (Prague, Czech Republic) [11–14]. All the data are consistent with the concept of EPR effect, and show that polymers with a molecular weight above 40 kDa exhibited prolonged plasma residence time and preferential accumulation of the polymeric or macromolecular drugs in the tumor tissue [11–16] (Figure 3.1).

Meanwhile, the EPR effect is applicable to a wide range of biocompatible macromolecules, such as proteins/antibodies, liposomes, micelles, DNA or RNA polyplexes, nanocarriers, and lipidic particles for cancer-selective drug delivery [13–16]. The number of papers that cite the EPR effect has increased in a logarithmic manner in recent years, reaching close to 8000 in 2010 (Figure 3.2). In this chapter, I will review the EPR effect briefly, and discuss problems/limitations, solutions, and further augmentation of the EPR effect.

3.2
What is the EPR Effect: Mechanism, Uniqueness, and Factors Involved

The EPR effect is a phenomenon resulting from multiple causes and effects, such as anatomical defects in vascular architecture and higher vascular density as a result of active production of angiogenic factors, especially when tumors are at an early stage and express growth factors such as vascular endothelial growth factors (VEGFs) and nitric oxide (NO). Many vascular permeability factors such as NO (Figure 3.3a–c), bradykinin, prostaglandins, collagenases, matrix metalloproteinases (MMPs), and so on, are overproduced in the tumor tissues (Tables 3.1 and 3.2). They facilitate extravasation of macromolecules in solid tumors [11–21]. As a result, more excessive tumor-selective vascular leakage of

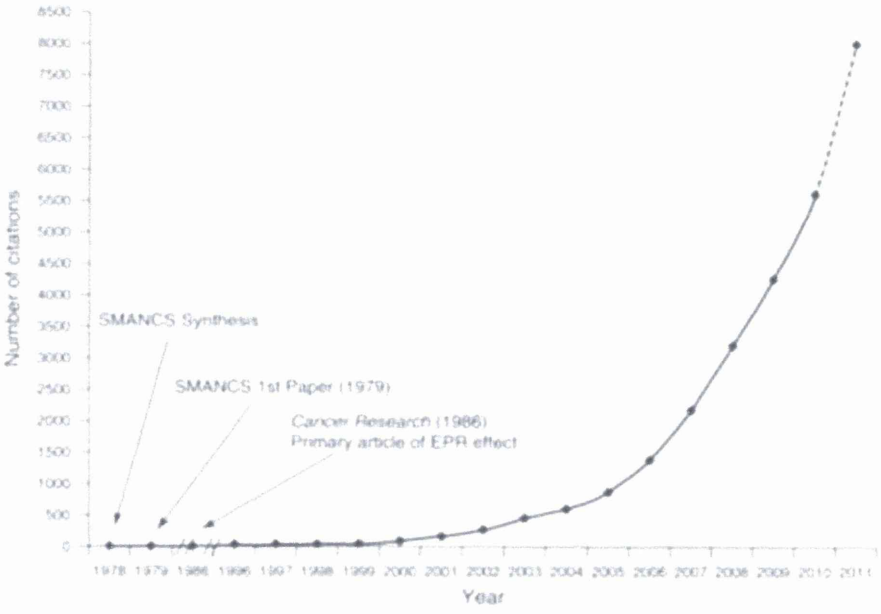

Figure 3.2 Citation numbers of the EPR effect and invention of the first polymeric drug, SMANCS (from *Science Direct* and *SciFinder*). (Adapted from [16].)

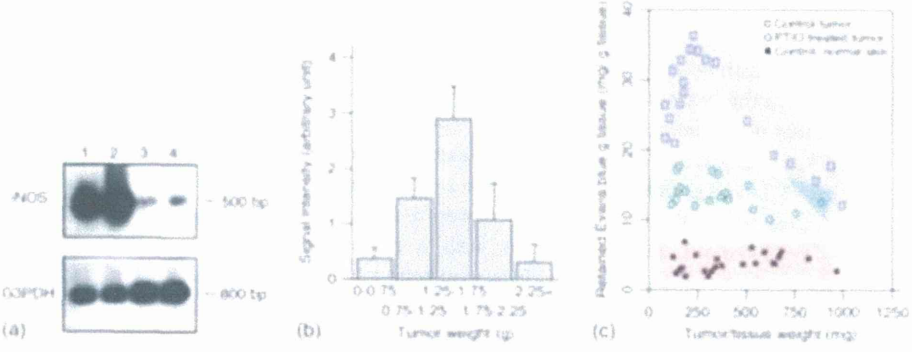

Figure 3.3 (a)–(c) Involvement of NO in the EPR effect: nitric oxide synthase (NOS) induction, relation to tumor size, and effect of NO scavenger by tumor size. (a) Upregulation of the inducible form of NOS (inducible nitric oxide synthase, iNOS) in tumors (lanes 1 and 2) and normal tissues (lanes 3 and 4). (b) Amount of NO generated in solid tumor (S 180) in mice as measured by electron spin resonance spectroscopy with dithiocarbamate–Fe complex and the relation to the size of tumor. (c) Amount of Evans blue–albumin permeation (EPR effect) and effects of NO scavenger (2-phenyl-4,4,5,5-tetramethylimidazoline-oxyl 3-oxide (PTIO) ○) or NOS inhibitor (■) in mouse tumors based on tumor size. Lower zone: control normal tissue; middle zone: treated with PTIO; top zone: control tumor, without NO scavenger. (Adapted from [16, 19].)

Table 3.1 Factors affecting the EPR effect of macromolecular drugs in solid tumors (extensive production of vascular mediators that facilitate extravasation)

Bradykinin
Nitric oxide (NO)
Vascular permeability factor/VEGF
Prostaglandins
Collagenase (MMPs)
Peroxynitrite ($ONOO^-$)
Anticancer agents
Inflammatory cells and H_2O_2
Heme oxygenase-1 (CO)

Table 3.2 Architectural differences and functions

1) Active angiogenesis and high vascular density
2) Defective vascular architecture
lack of smooth muscle layer
lack of or fewer receptors for angiotensin II
large gap in endothelial cell–cell junctions and fenestration
anomalous conformation of tumor vasculature (e.g., branching or stretching)
3) Defective lymphatic clearance of macromolecules and lipids from interstitial tissue (prolonged retention of these substances)
4) Whimsical and bidirectional blood flow

an albumin-bound dye such as Evans blue will occur only at the tumor site, as seen in the examples shown in Figure 3.1a. The uniqueness of this phenomenon is that it will be only seen in tumor tissues, but not in the normal healthy tissue [11, 13–20]. Obviously, normal vasculatures shows no such leakage (Figures 3.1a and 3.3a and c) due to their complete architecture of the blood vasculature as well as little production of vascular mediators as listed in Table 3.1.

Furthermore, macromolecules with a molecular weight more than 40 kDa above the renal threshold such as synthetic polymers, serum proteins, micelles, polymer-based or lipid-based nanoparticles that leak out of the blood vasculature into the interstitial space of tumor tissues remain there for a very long time, even for several weeks, without being cleared (Figures 3.1a,b 3.4, 3.5, and 3.9b) [1, 13, 15]. In contrast to tumors, such micro- or nano- particles, should they leak out of the blood vasculature into normal tissue, will be cleared gradually by the lymphatic system in several days as is usually seen for common inflammations of normal tissue. Neovasculature generated by the tumor is characterized by an irregular shape, dilated, leaky, or defective vessels. The endothelial cells are poorly aligned or disorganized with large fenestrations as illustrated for healthy and tumor vessels in Figure 3.4.

These anatomical features make the vasculature of tumor tissue permeable for macromolecules or even larger nanosized particles such as liposomes or polymeric micelles, whereas in blood vessels of healthy tissue only small molecules can pass

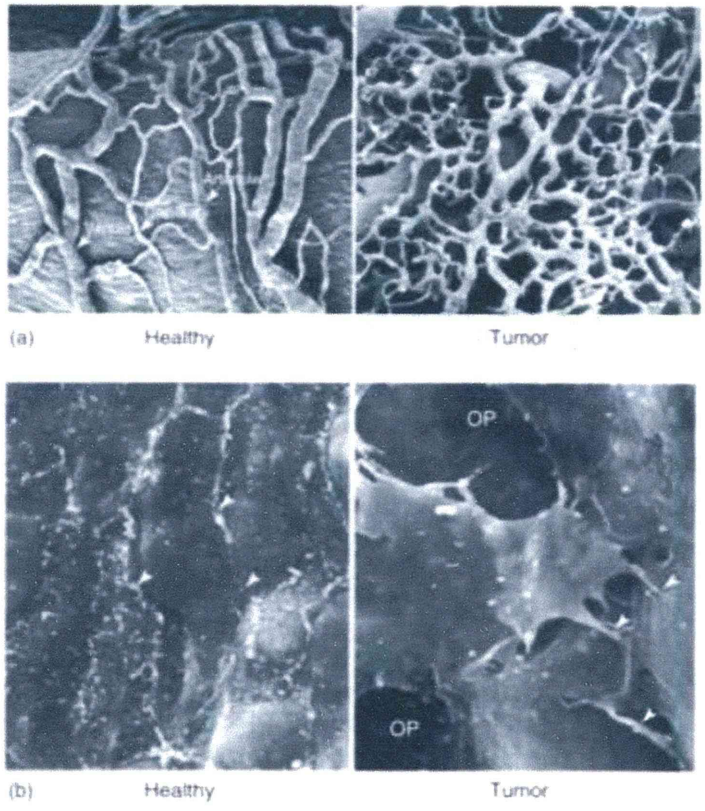

Figure 3.4 (a) Scanning electron microscopy (SEM) imaging of polymer casts of normal (vasa vasorum of rat carotid sinus, left) and tumor (xenograft of human head and neck cancer in nude mouse, right) microvasculature. Marked differences are found in the degree of organization and an apparent lack of conventional hierarchy of blood vessels of the tumor sample. (b) SEM images of the luminal surface of healthy (mouse mammary gland, left) and tumor (MCa-IV mouse mammary carcinoma, right) blood vessels. While the healthy vessel is smooth and has tight endothelial junctions (arrow heads), the tumor vessel shows widened intercellular spaces, overlapping endothelial cells (arrow heads), opening (OP) and other abnormalities. (Reproduced with permission from [22].)

the endothelial barrier. The pore size of tumor microvessels was reported to vary from 100 to 1200 nm in diameter (depending on the anatomic location of the tumor). In contrast, the tight junctions between endothelial cells of microvessels in most normal tissues are less than 2 nm in diameter (noteworthy exceptions are found in postcapillary venules (up to 6 nm), and in the kidneys, liver, and spleen (up to 150 nm)) Figure 3.4b.

The EPR effect is depicted schematically in Figure 3.5.

Figure 3.5 illustrates that blood vessels in most normal tissues have an intact endothelial layer that allows the diffusion of small molecules, but not the entry of

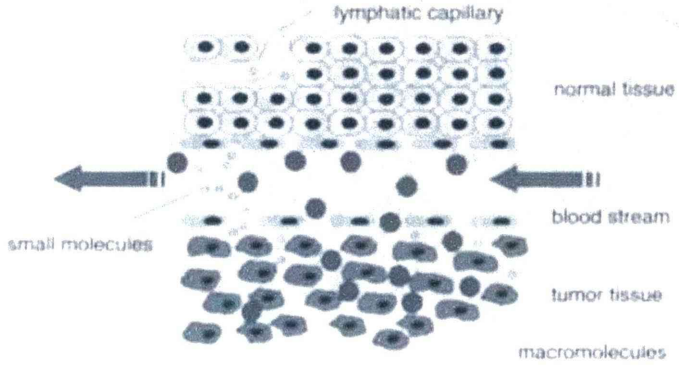

Figure 3.5 Schematic representation of the anatomical and physiological characteristics of normal (upper half) and tumor (lower half) tissues with respect to the vascular permeability and retention of small (lighter circles) and large molecules (darker circles) (see text) [23]

macromolecules into the tissue. In contrast, the endothelial layer of blood vessels in tumor tissue is often leaky so that small as well as large molecules have access to malignant tissue. As tumor tissue does not generally have a lymphatic drainage system, macromolecules are thus retained and can accumulate in solid tumors.

As described above, we can demonstrate this retention effect by injecting Evans blue intravenously, which binds with high affinity and selectivity to the plasma protein albumin (66.5 kDa), and remains in circulation for more than several hours in rodents.

During the long circulation time of Evans blue bound to albumin, the albumin–Evans blue complex will eventually permeate through the porous tumor blood vessels into the interstitial tissue of tumor, thus staining the tumor blue (Figure 3.1a, 3.5). Alternatively, by infusing a lipid contrast agent such as Lipiodol® with/without the polymeric anticancer drug SMANCS (a conjugate of SMA and NCS) via the tumor-feeding arterial route, Lipiodol will be taken up most effectively by the tumor (Figure 3.6a,c and 3.7). In this case, the ratio of the concentration of Lipiodol in the tumor to circulating blood is more than 2000-fold, translating into an extremely tumor pin-pointed targeted delivery [24–26]. When X-ray computed tomography (CT) scans are taken 1 or 2 days after Lipiodol infusion, one can visualize the white Lipiodol-stained tumor areas showing tumor-selective extravasated areas (Figure 3.7a). In this setting, the lipophilic polymeric drug SMANCS dissolved in Lipiodol (thus named SMANCS/Lipiodol) is retained in the tumor tissue selectively. The presence of Lipiodol and SMANCS can be detected as high-electron-density areas ("white areas") due to iodine in Lipiodol using X-ray imaging [14, 24–26].

This method allows detection of tumor nodules as small as a few millimeters in diameter [24, 25]. Furthermore, this prolonged retention in tumor tissue is more than just a passive targeting. Namely, when a low-molecular-weight water-soluble contrast agent is infused under identical conditions (known as angiography)

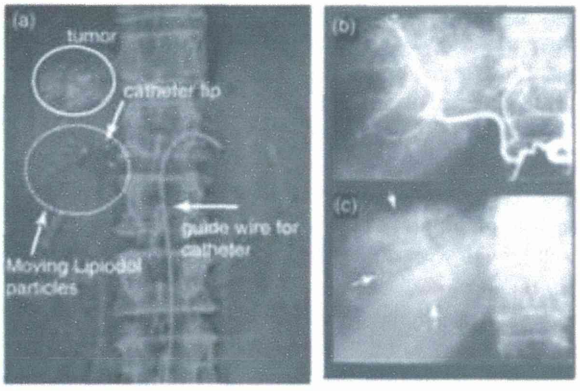

Figure 3.6 (a) Angiographic arterial infusion of SMANCS/Lipiodol using a catheter (Seldinger method) via the hepatic artery (where vascular leakage is seen, but only within 1 min). White Lipiodol particles coming out are captured at the tumor. (b) Arterial phase (blood vessels are visible). (c) Venous phase.

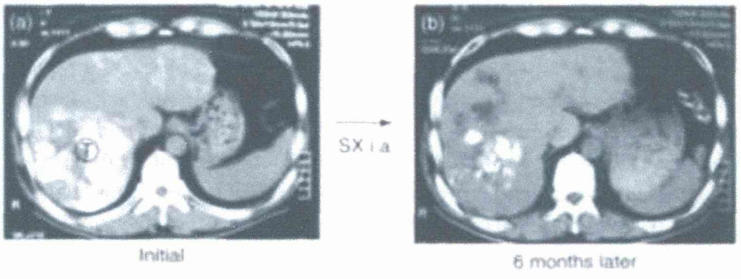

Figure 3.7 X-ray CT scan images of hepatocellular carcinoma (hepatoma) of a patient, where tumor location 'T' and size are visualized by white staining of high-electron-density iodine in the radio contrast agent Lipiodol, which is selectively retained in the tumor. (a) CT image at the first injection. (b) Significant size reduction of the tumor is seen after 6 months of arterial injection of SMANCS 3 times in 6 months via the hepatic artery.

(Figure 3.6a and b) it allows visualization of a solid tumor with the aid of X-ray imaging. However, this tumor staining lasts for only 1–5 min as illustrated by venous-phase staining images (e.g., Figure 3.6c). In contrast to this short time of duration, lipid particles (e.g., Lipiodol) or polymeric drugs or albumin-bound Evans blue are retained for significantly longer time periods as a result of the EPR effect. The prolonged retention of macromolecules and nanoparticles in the tumor continues for days to weeks, and if they carry a drug this can be released in the vicinity of tumor cells. When an adequate concentration of the active drug in the tumor tissue is attained, it will lead to definite tumor regressions [27]. Thus, the EPR effect is an event observed in *in vivo* settings, but not *in vitro* or cell-free systems, not to mention in normal tissues.

In this context, it may be worth mentioning the enhanced vascular permeability of inflammatory tissues. The enhanced vascular permeability of a tissue is one of the hallmark manifestations of inflammation, which may also involve bradykinin, reactive oxygen species, and other mediators. We had initially observed that bacterial proteases induce activation of a bradykinin-generating cascade [28–32]. Similar events were also discovered in cancer tissues [20, 21, 29–32]. Activation of the kallikrein–kinin cascade leads to the generation of bradykinin that will potentiate the EPR effect instead of suppressing the EPR effect. Another effect is the heterogeneous tumor cell growth with unparalleled angiogenesis resulting in inadequate supply of oxygen (i.e., low pO_2), which will affect induction of p53 or other events that will lead to apoptosis signaling, including the disappearance of vasculature or apoptotic/necrotic tissue death.

If the tumor tissue retained normal or near normal innate immunity such as macrophage functions, it would exert defensive a host response generating NO and superoxide (O_2^-). Both of them react immediately to become peroxynitrite ($ONOO^-$) at confined local vicinities, where $ONOO^-$ is highly toxic and exerts oxidative and nitrating effect, and affects cancer cells [29]. In addition to the cytotoxic effect of $ONOO^-$ (and ClO^-), $ONOO^-$ can activate MMPs (or collagenases) that disrupt tissue matrices and vascular integrity, and facilitate vascular leakage (i.e., the EPR effect) [19, 20, 29, 33]. (The $ONOO^-$ thus generated modifies tyrosine to form nitrotyrosine and guanine to form 8-nitroguanine in nucleic acid as well as 8-nitrocylic GMP [34, 35]. 8-Nitroguanosine becomes a substrate of NADPH-dependent reductase such as cytochrome b_5 reductase and iNOS [36, 37]. As a matter of fact, one can demonstrate the presence of nitrotyrosine and 8-nitroguanosine in tumor cells (by fluorescence immunostaining and high-performance liquid chromatography). The cell-killing potency of $ONOO^-$ is as strong as hypochlorite (ClO^-; i.e., below 10 μM), which is another reactive chemical produced by leukocytes (neutrophils) from H_2O_2 and Cl^- by myeloperoxidase [29].) Tumor tissues under these circumstances are therefore heterogeneous or different from normal pathophysiological tissue.

These vascular effectors that are common among cancer and inflammatory tissues open up the endothelial cell–cell junction, and allow proteins and macromolecules to extravasate into the interstitial tissue. However, they will be gradually recovered via the lymphatic clearance system in a matter of a few to several days. In contrast to this phenomenon of normal tissue, the clearance of drug nanoparticles or drug polymer conjugates from cancer tissue is much slower, and results in sustained access of this type of polymer therapeutics to cancer cells, which is the most desired goal in cancer drug delivery.

3.3
Heterogeneity of the EPR Effect: A Problem in Drug Delivery

The EPR effect is universally observed in rodent, rabbit, and human solid tumors. It is more typical when the tumor size is less than 1 cm. However, as shown in Figure 3.8a–c, when a tumor grows larger than 1 cm, the tumor exhibits more heterogeneity in the EPR effect. Yet it is seen even when tumor nodules are as

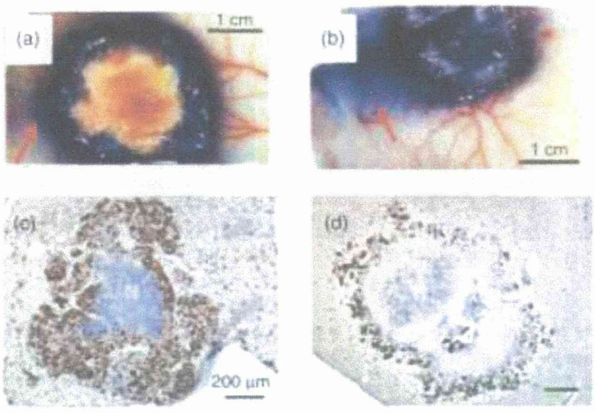

Figure 3.8 Heterogeneity of the EPR effect as seen by extravasation of Evans blue–albumin in tumor. (a) and (b) S-180 tumor in mouse. Macroscopic tumor and the skin, after intravenous Evans blue injection. In both (a) and (b), the tumor tissue shows heterogeneous staining of Evans blue as inhomogeneous extravasation of the blue dye–albumin complex. This type of peripheral uptake of SMANCS/Lipiodol is seen via CT in metastatic human tumors and is classified as B-type staining [26]. Arrows in (a) and (b) point to areas in which the EPR effect also occurs in normal tissue as a result of the generation of vascular mediators such as bradykinin. This extravasated blue albumin in normal skin will be cleared via the lymphatics. Ki-67 immunohistochemistry was used to assess tumor proliferation in (c) and (d). Proliferating cells were demarcated by intense brown diaminobenzidine staining in (c). In (d), polymeric drug SMA–pirarubicin reduced tumor proliferation by greater than 75% in 72 h after one intravenous injection. Control tumors of (c) demonstrated a high degree of tumor proliferation. Tumor proliferation was restricted to a thick viable band at the tumor periphery with significant central necrosis (N). (d) Proliferation in SMA–pirarubicin-treated tumors was restricted to the thin viable rim at the tumor periphery. Scale bars = 200 µm [38].

small as 0.5 mm in diameter in metastatic micronodules of the liver (Figure 3.8c,d), although tumor-selective extravasation of a polymeric drug (by the EPR effect) can be observed (Figure 3.9b). In the metastatic liver cancer model of colon cancer, the microheterogeneity of the EPR effect is also observed as viable parts and necrotic parts near the center of the tumor (Figure 3.8c) [38]. However, it should be noted that the tumor-proliferating area is located primarily at the periphery of the solid tumor, which coincides with the area showing an extensive EPR effect, while a hypovascular or avascular appearance is seen in the tumor center (Figures 3.8a and c and 3.10a and b). Despite the heterogeneity of the EPR or the vasculature of the tumor, macromolecular drugs show much more drug accumulation by EPR in the tumor periphery where more proliferating tumor cells exist (see peripheral staining in Figures 3.8a and c and 3.10a,b).

Therefore, the area with a high EPR effect coincides with the tumor growth area. Thus, using cytostatic polymeric drugs is more advantageous from the therapeutic point of view since they act effectively on proliferating cancer cells. In this context, 90–95% suppression of metastatic tumor nodules in the liver by

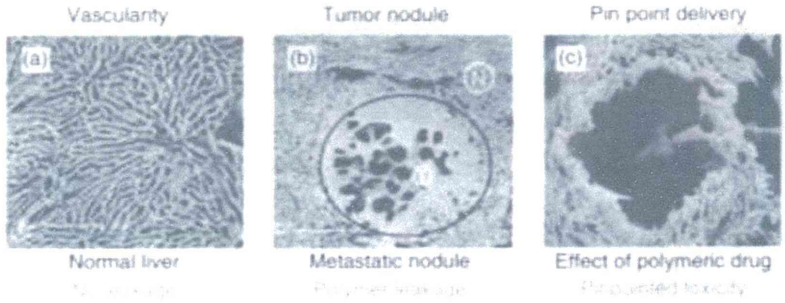

Figure 3.9 SEM images of metastatic colon cancer to the liver. (a) Normal liver vessels. (b) Metastatic micronodule of tumor indicating by 'T' (blood bed) where polymeric resin is extravagated by the EPR effect. (c) After a treatment of tumor selective polymeric drug (SMA micelles with pirarubicin) by intravenous injection. The nodular blood bed of the metastatic tumor has disintegrated. tumor tissue has undergone apoptosis and necrosis by tumor-selective drug delivery; however, no damage to the normal liver tissue is seen. More than 95% of tumor nodules in the liver are destroyed by this drug given intravenously. The images are courtesy of Dr. J. Daruwalla and Professor C. Christophi of the University of Melbourne, Australia [38].

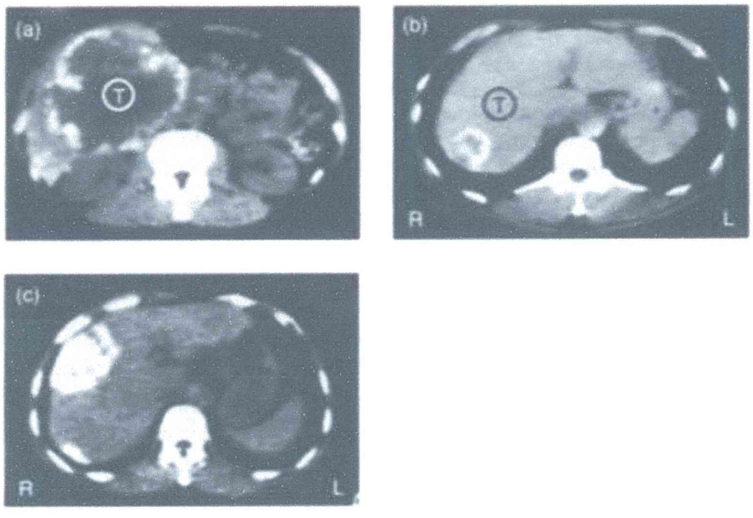

Figure 3.10 X-ray CT scan of the liver cancer after SMANCS/Lipiodol injection via the arterial route under normotensive blood pressure. Heterogeneity of drug uptake in (a) and (b) is remarkable as a ring-like staining. Namely, an avascular or hypovascular area is noted as a dark area in the central part of metastatic liver cancer (a), a massive size metastasized tumor from the gallbladder, and (b) metastatic liver cancer from the colon. In (c), primary liver cancer (hepatocellular carcinoma) seen as a white area at the right side of the liver lobe in the CT image where uptake of SMANCS/Lipiodol is homogeneous.

single intravenous injection of SMA–pirarubicin micelles was significant and a promising result for future drug design in this area of research [38].

In relation to the heterogeneity of the EPR effect, most metastatic tumors in the liver in human patients show hypovascular properties near the tumor center as shown in Figure 3.10. Figure 3.10a is a massive metastatic gallbladder cancer to the liver that shows much less drug (SMANCS/Lipiodol) uptake in the central area when given intra-arterially under normotensive conditions. We have defined these CT images of centrally hypovascular or avascular staining (low density even after Lipiodol infusion) as type B staining [26]. In Figure 3.10b, small-sized metastatic liver cancer originating from the colon in the right lobe also show B-type staining. In contrast, hepatocellular carcinoma (or primary liver cancer) and renal carcinoma usually exhibit complete filling of SMANCS/Lipiodol after arterial infusion under normotensive conditions, and the entire tumor is stained without a central low-density area (Figure 3.10c). This staining was defined type A staining by CT scans, and usually exhibits more homogeneous staining and a good EPR effect [26]. Type A staining is a common feature of tumors with high vascular density such as hepatocellular carcinoma and renal cell carcinoma. Prostate and pancreatic cancers, conversely, show low-density staining, indicating less potential for drug delivery, thus, augmentation of EPR effect is needed as described below.

3.4 Overcoming the Heterogeneity of the EPR Effect for Drug Delivery and How to Enhance the EPR Effect

3.4.1 Angiotensin II-Induced High Blood Pressure

To counteract the heterogeneous EPR effect of hypovascular tumor tissue as described above, which shows reduced drug delivery, we have developed two methods to enhance tumor drug delivery and overcome the problem of EPR-less-dependent tumor tissue. One method is by elevating the blood pressure during the arterial infusion of macromolecular drugs by using angiotensin II (a vasoconstrictor). This can be achieved, for instance, by increasing the systolic blood pressure from 90–120 to 150–160 mmHg and maintaining the hypertensive state for 15–20 min [27, 39, 40]. As shown in Figure 3.11a and b, by angiography of the same experimental rat tumor (window model), the angiotensin-induced hypertension allows the visualization of significantly more blood vessels that are otherwise not visible (Figure 3.11a vs b) [39, 40].

Despite an apparently avascular large tumor mass as shown in Figure 3.11c, e, and g, delivery of SMANCS/Lipiodol was significantly augmented as seen in Figure 3.11 (d, f, and h, respectively). SMANCS/Lipiodol can be delivered effectively to the tumors (see below) and remarkable regression was obtained. It should be noted that when angiotensin II is applied intravenously by slow infusion, blood

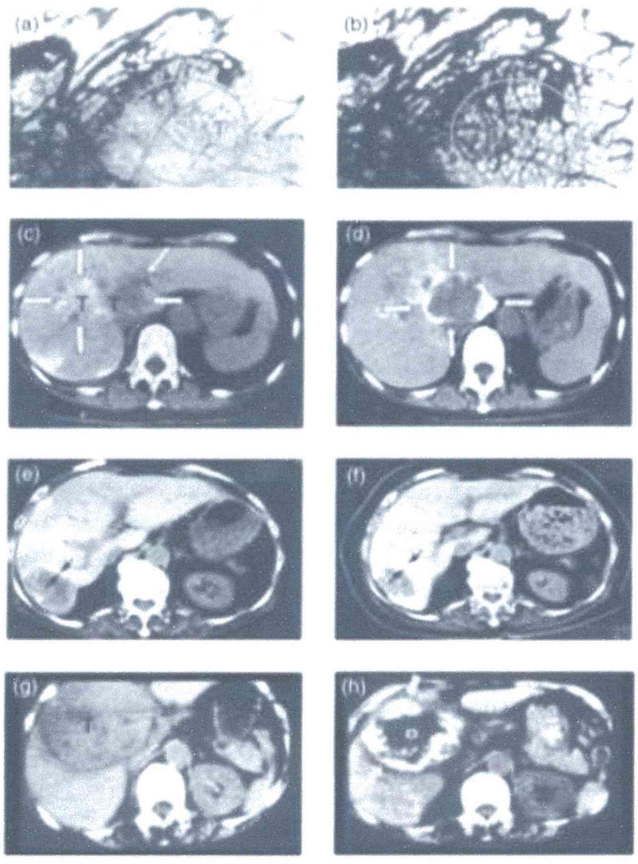

Figure 3.11 Augmentation of the EPR effect by angiotensin II-induced high blood pressure. (a) and (b) Window chamber model of an experimental rat tumor model. Blood vessels are only weekly seen under the normotensive state (circled area) in (a), but the blood vessels became dense as noted in (b) when the systolic blood pressure of 90 mmHg was elevated to 160 mmHg (circled area). (Adapted from [39].) The following examples are results of arterial infusion of SMANCS/Lipiodol of normotensive blood pressure (90–120 mmHg) (c, e, and g) and angiotensin II-infused conditions (to about 150–160 mmHg) (d, f, and h). (c)–(f) Colon cancer → liver metastasis. (g) and (h) a case with massive gallbladder cancer metastasized to the liver. In all these (c, e, and g) difficult-to-treat cases, angiotensin-induced a hypertensive state and clearly showed significantly enhanced drug delivery (see arrows, white area).

flow volume increased selectively in the tumor, whereas all normal tissues exhibit a constant blood flow volume regardless of the blood pressure applied [40].

Under this condition, drug delivery to tumor tissue was increased selectively as seen by Evans blue complexed with albumin or radiolabeled albumin. There seems less delivery to normal tissues under this hypertensive condition [41]. Thus, fewer side-effects were seen than in the normotensive state (as revealed by blood cell

count, diarrhea, or liver and kidney functions), while this method resulted in a marked increase of drug delivery to the tumor by a factor of 2–3 [41].

In parallel to this increased EPR effect and concomitant drug delivery, we observed an improved therapeutic effect as well as decreased adverse toxicity. This remarkably improved therapeutic effect was observed not only in the rat model, but more importantly also in human patients with difficult-to-treat tumors, such as metastatic liver cancer, pancreatic cancer with liver metastases, massive renal cancer, cancer of the gallbladder with liver metastases, and cholangiocarcinoma [27] (Figure 3.12).

In light of these encouraging results, the next key issue is to optimize the release rate of the drug to attain a drug concentration above the IC_{50} value (inhibitory dose of 50% cell kill) or the minimum inhibitory concentration. SMANCS/Lipiodol of

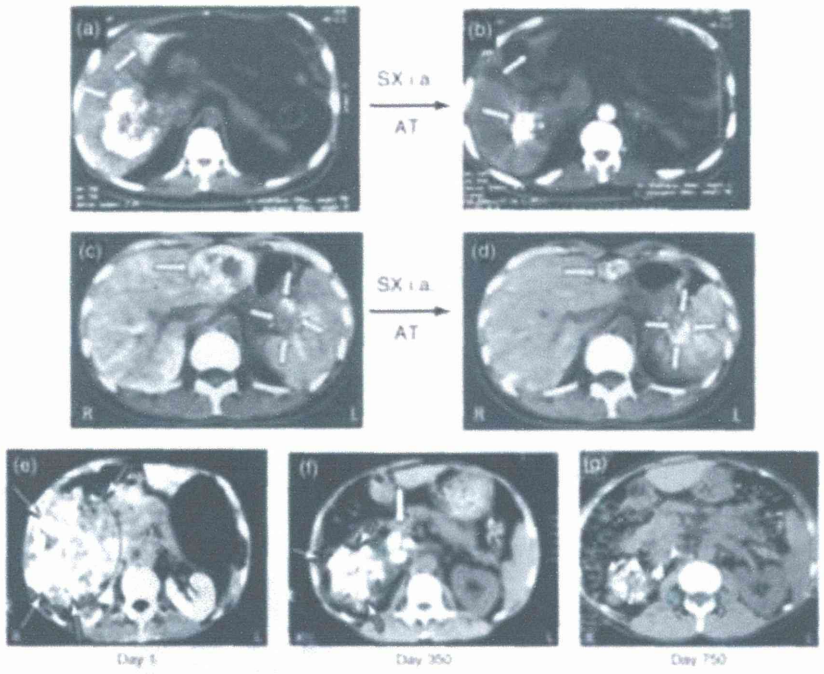

Figure 3.12 Enhanced drug delivery under angiotensin-induced high blood pressure and remarkably improved therapeutic outcome. (a) and (b) A massive metastatic liver cancer originated from stomach cancer regressed considerably in 50 days. It was injected under an angiotensin II-induced hypertensive state. Almost complete filling of the drug (SX) inside the tumor and tumor-selective drug deposition is seen. The white area indicates SMANCS/Lipiodol. (c) and (d) Metastatic liver cancer from a pancreatic cancer. It was similarly treated with SMANCS/Lipiodol given intra-arterially. Both metastatic tumors in the liver and primary tumors in the pancreas regressed considerably within a few months. (e)–(g) Massive renal cell carcinoma treated with SMANCS/Lipiodol similarly regressed remarkably and this patient is still healthy with good a quality of life (longer than 8 years). (From [27].)